

The Effect of Pretreatment Method on the Preparation of Micro-mesoporous ZSM-5/ γ -Al₂O₃ Composite Materials

CHU Ruizhi^{1,2, a*}, XU Tingting^{1,b}, MENG Xianliang^{1,2,c} and HOU Wenxin^{1,d}

¹ School of Chemical Engineering, China University of Mining & Technology, Xuzhou, Jiangsu, China 221008

² High-Tech Research Institute Of China University of Mining and Technology, Lianyungang, Jiangsu, China 222000

^axttcumt@163.com, ^bjennifer_crz@163.com, ^ckevin-meng@163.com, ^d18242311143@163.com

Abstract. A series of ZSM-5/ γ -Al₂O₃ composite materials were prepared under various pretreatment method; The physicochemical properties of composite materials were investigated by XRD, SEM, FTIR to find out optimal pretreatment method. The results showed that the composite materials performance better structure property when γ -Al₂O₃ was firstly immersed in TPAOH solution under reflux condensation for a period of time and then immersed into anhydrous alcohol before mixed with ZSM-5 precursor solution. The result of infrared spectrum indicated that the formation of Al-OH bond played a key role in the synthesis of micro-mesoporous ZSM-5/ γ -Al₂O₃ composite materials.

Keywords: γ -Al₂O₃; pretreatment method; TPAOH; ZSM-5/ γ -Al₂O₃; micro-mesoporopus

1 Introduction

Micro-mesoporous materials have interconnected pores with double model pore distribution of micropore and mesopore combined the advantages of mesoporous materials and the strong acidity and high thermal stability of microporous molecular sieves[1-4]. It can be predicted that it has good development prospect to be used as catalyst carrier in catalytic hydrogenation desulfurization[5-8]. The introduction of microporous secondary structure units into pore walls of mesoporous is a key problem in the preparation of micro-mesoporous materials. It is core factor to obtain stable performance catalyst with specific pore size distribution and excellent sulfur tolerance[9,10]. Micro-mesoporous materials have been paid much attention since micro-mesoporopus MCM-41/FAU materials were synthesized in one step by Kloetstra et al. in 1996[11]. Preparation of micro-mesoporopus composite molecular sieve with microporous molecular sieve as the skeleton is one of the important methods to obtain composite materials. Zhao[12] adopted two-step hydrothermal crystallization method to synthesize micro-mesoporopus composite molecular sieve(M β).

* Corresponding author: xttcumt@163.com

Triantafyllidis et al.[13,14], Van Oers et al.[15], Di et al.[16,17] and Zheng[18, 19] have studied introducing primary or secondary structure of microporous molecular sieve such as ZSM-5, β into pore walls of mesoporous molecular sieve to synthesize micro-mesoporous composite materials successfully. The pore and crystal structure of γ - Al_2O_3 can be kept stable under the crystallization conditions of ZSM-5 molecular sieve, and they all belong to alumina material. However, the aluminosilicate gel of ZSM-5 can not be dispersed in gamma- Al_2O_3 structure effectively. In this paper, we prepared a series of micro-mesoporous ZSM-5/ Al_2O_3 composite materials under different pretreatment method. To choose optimal pretreatment method by analysis the result of XRD, nitrogen adsorption - off desorption isotherms, BET specific surface area, SEM.

2 Experimental

2.1 Samples Preparation

Pretreatment method A1: γ - Al_2O_3 powder was mixed with TPAOH in the mass ratio of 25%, by certain solid-liquid ratio, washing and filtering the mixture after heating and immersion for a period of time under reflux condensation, then dipped it into anhydrous alcohol for a period of time and then filtered it again, washed two or three times and dry it.

Pretreatment method A2: Following the same process to pretreatment method A1, without dipping it into anhydrous alcohol for a period of time.

Pretreatment method A3: γ - Al_2O_3 powder was impregnated into the TPAOH solution at room temperature for 4 h, then washed and dry it.

Respectively 5 g γ - Al_2O_3 pretreated under pretreatment method A1, A2, A3 were impregnated into 30 ml molecular sieve precursor solution (mole ratio: 150SiO_2 : Al_2O_3 : $13.5\text{Na}_2\text{O}$: 20TPAOH : $3000\text{H}_2\text{O}$) in a crystallization reactor at $120\text{ }^\circ\text{C}$ for 4 h, and then crystallized at $180\text{ }^\circ\text{C}$ for 24 h. The samples after crystallization were filtered and washed until pH value was less than 8, and then the composite materials were dried under $100\text{ }^\circ\text{C}$ for 24 hours. With $1\text{ }^\circ\text{C}/\text{min}$ heating rate rose to $550\text{ }^\circ\text{C}$ in air atmosphere, the samples were calcinated for 6 hours at $550\text{ }^\circ\text{C}$. The synthesized materials were named as YFA1, YFA2 and YFA3 corresponding to pretreatment method A1, A2, A3. YFA0 represented γ - Al_2O_3 without pretreatment.

2.2 Characterization

X-ray diffraction (XRD) patterns of the samples were recorded on a Bruker D8 ADVANCE diffractometer using Cu $K\alpha$ radiation. The X-ray tube was operated at 40 kV and 30 mA, and its scanning range and scanning rate were 3° - 80° , $2^\circ/\text{min}$ respectively. The textural properties of supports and samples were determined from the nitrogen adsorption/desorption isotherms at 77 K, using a fully automated Quantachrome Autosorb-1 gas adsorption device. The isotherms were elaborated according to the Brunauer-Emmett-Teller (BET) method for surface area calculation, pore size distribution was determined by NLDFT method. SEM was performed with an FEI Quanta TM-250 scanning electron microscope to observe surface morphology of the samples. Scanning electron microscope was operated at 0.2kV-30 kV, resolution value was 22 nm (High vacuum mode). Infrared Spectrum patterns of the samples were recorded on a USA Nicolet Nexus470 infrared spectrometer using KBr pellets. FT-IR characterization were carried out as follows: Test samples with KBr (chromatography pure) were dried at $105\text{ }^\circ\text{C}$ for 2 h, subsequently cooled to room temperature in dryer. 2mg specimens and 300 mg KBr were

grinded in mortar agate until the particle size was less than 2 μm to prevent light scattering effect. Then a certain amount of mixed powder were pressed into a transparent wafer into the infrared test mould for test.

3 Results and Discussion

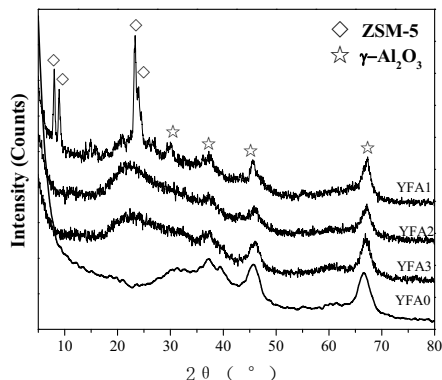


Fig. 1 X-ray diffraction patterns of samples: YFA0 ($\gamma\text{-Al}_2\text{O}_3$ without pretreatment); YFA1 (pretreatment method A1); YFA2 (pretreatment method A2); YFA3(pretreatment method A3)

3.1 XRD Patterns Analysis.

The XRD patterns of samples prepared under different pretreatment methods were presented in Fig. 1. The patterns of Samples YFA2 and YFA3 showed well-resolved diffraction peaks, which were well matched to $\gamma\text{-Al}_2\text{O}_3$ -type structure diffraction peaks at 66° , 45° , 39° and 32° 2θ . However, the characteristic peaks of ZSM-5 structure ($5\sim 8^\circ$ and $23\sim 25^\circ$ 2θ) were not observed obviously, where only small “steamed bread” peak could be seen, suggesting that ZSM-5 crystal phase structure could not generated well on $\gamma\text{-Al}_2\text{O}_3$ with these two kinds of pretreatment method[20]. The patterns of Samples YFA1 showed the characteristic reflection peak of ZSM-5 (two strong diffraction peak at $5\sim 8^\circ$ 2θ along with obvious characteristics of the finger peak at $23\sim 25^\circ$ 2θ), meanwhile the four strongest diffraction peak of $\gamma\text{-Al}_2\text{O}_3$ were observed and there was a diminution of $\gamma\text{-Al}_2\text{O}_3$ peaks intensities with enhancement of the ZSM-5 peaks, suggesting micro-mesoporous materials ZSM-5/ $\gamma\text{-Al}_2\text{O}_3$ could be synthesized under pretreatment methods A1. Thus it can be seen that pretreatment method had a great influence on the synthesise of the composite materials and the product crystallization.

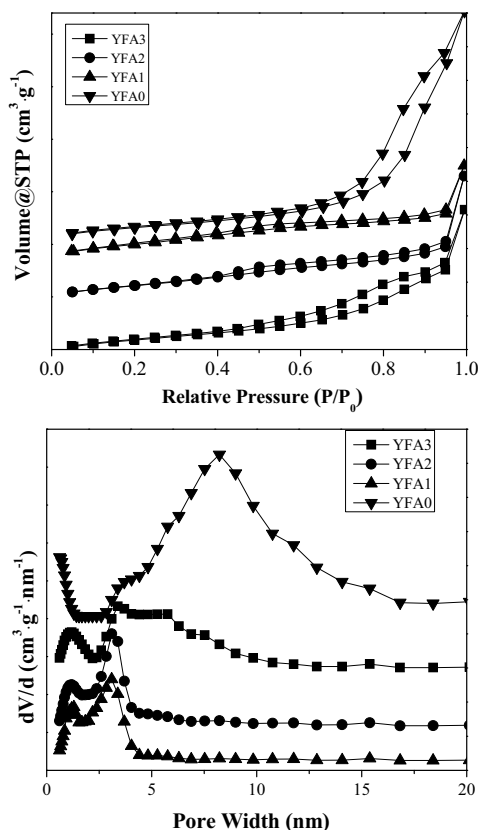


Fig. 2 Adsorption-desorption isotherms (a)-Pore diameter distribution (b) of samples: YFA0 (γ - Al_2O_3 without pretreatment); YFA1 (pretreatment method A1); YFA2 (pretreatment method A2); YFA3(pretreatment method A3)

3.2 Surface Properties Analysis.

The N_2 adsorption-desorption isotherms of samples YFA0, YFA1, YFA2, YFA3 were presented in Fig.2-a. The isotherm of YFA0 exhibited the isotherms of Langmuir type IV, moreover, the shape of the hysteresis loops of supports fell within the H3 category, appeared as a typical mesoporous adsorption-desorption isotherm. The isotherm of samples YFA1, YFA2 and YFA3 exhibited the isotherms of Langmuir type IV. However, when the relative pressure $P/P_0 < 0.4$, the adsorption quantity was smaller while the H4 type hysteresis loop appeared and adsorption quantity increased obviously under relative pressure P/P_0 range from 0.4 to 1.0, indicating the existence of micro-mesoporous structures. When P/P_0 approached to 1, saturated adsorption platform were not observed, indicating that were not single orderly arrangement channels, which further proved the materials were micro-mesoporous materials. Adsorption quantity of sample YFA3 was the largest, which was due to its largest specific surface area. Unfortunately, adsorption isotherm platform of sample YFA3 was small under medium relative pressure, showing pore size distribution was heterogeneous. A platform of sample YFA1 and YFA2 was observed in the region of $0.4 < P/P_0 < 0.8$ proved pore diameter distribution were uniform.

In Fig 2-b the pore size distribution of YFA0 was mainly concentrated at 8 nm, which was typical mesoporous pore size distribution. Sample YFA1 had no obvious peaks of micropore, therefore it did not meet the requirements of micro-mesoporous materials. Both sample YFA1 and YFA2 were micro-mesoporous materials, however the aperture of sample YFA2 was mainly distributed in 5~7nm, the micropore is not obvious and the pore size distribution was relatively wide along with low order degree. The aperture of sample YFA1 was mainly distributed in 1nm and 4 nm around, and the pore size distribution was narrow, meanwhile the degree of order was improved, which fully indicated that the composite materials prepared by the pretreatment method of A1 had the porous structure of both microporous and mesoporous.

Table1 Textural Properties Of Samples

Sample	Pretreatment Method	specific surface area [m ² .g ⁻¹]	total pore volume [cm ³ .g ⁻¹]	mean pore size [nm]	specific surface area [m ² .g ⁻¹]		pore volume [cm ³ .g ⁻¹]	
					mesoporous	micropore	mesopore	micropore
YFA0		411.8	1.733	17.23	330.1	58.1	1.380	0.0173
YFA1	A1	203.6	0.3744	7.351	164.2	97.6	0.1786	0.0440
YFA2	A2	193.9	0.4844	9.996	177.6	56.2	0.2220	0.0260
YFA3	A3	202.6	0.5658	11.17	206.0	28.0	0.3580	0.0126

The results of textural properties of samples were shown in Table 1. The specific surface area of samples synthesized under pretreatment method decreased significantly compared with γ -Al₂O₃, which reflected part of channels collapsed and the structure were damaged to some degree. Compared with the other two pretreatment methods, sample YFA1 had larger specific surface area, microporous specific surface area and micropore volume while the total pore volume and average pore diameter were small. This is due to the loading of the microporous molecular sieve blocking part of the channels. Fortunately, the microporous specific surface area and micropore volume are much less than mesoporous, indicating that only a small amount of ZSM-5 were loaded in mesoporous γ -Al₂O₃, which would not hinder the advantages of mesoporous channel. To sum up, the micro mesoporous ZSM-5/ γ -Al₂O₃ composite materials were better under pretreatment method A1 in terms of the specific surface area and pore structure.

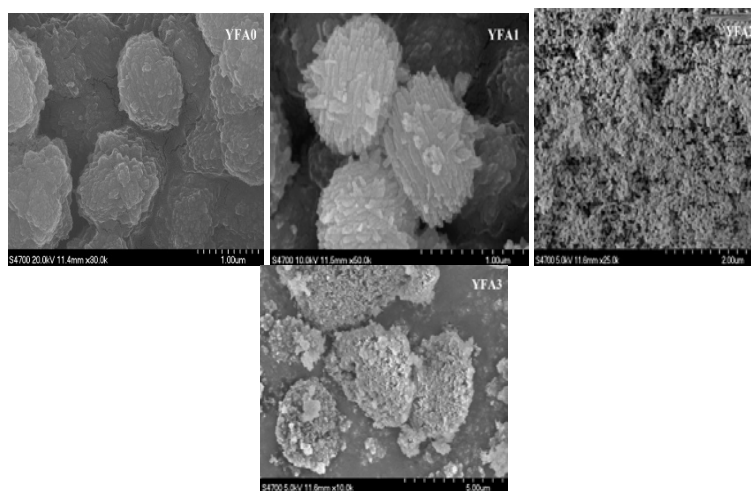


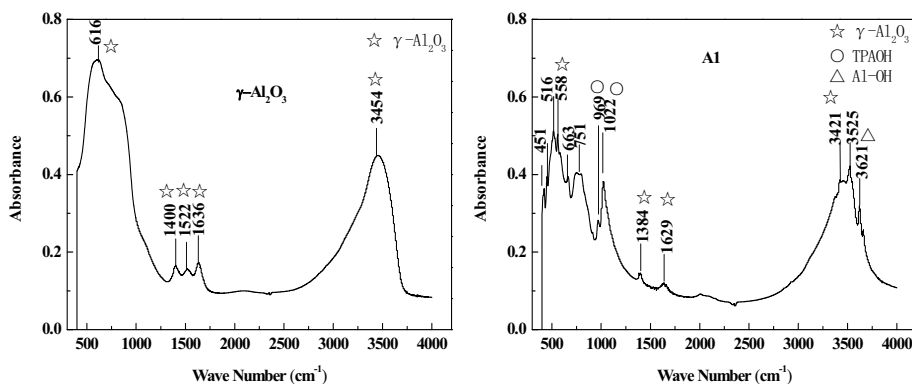
Fig. 3 The SEM images of samples :YFA0 (γ -Al₂O₃ without pretreatment); YFA1 (pretreatment method A1); YFA2 (pretreatment method A2); YFA3(pretreatment method A3)

3.3 SEM Analysis.

Fig. 3 illustrated the SEM images of samples synthesized under different pretreatment methods, among which YFA0 was the SEM images of mesoporous γ - Al_2O_3 without pretreatment. As was shown in the figures, pretreatment methods had a great influence on the morphology of composite materials. The morphology of YFA2 and YFA3 were in disordered state, combining to be flocculent and had no obvious crystal. γ - Al_2O_3 can hardly remain the original appearance may be due to the surface and inner channels of mesoporous γ - Al_2O_3 were excessive corrosion exceedingly by pretreating agent without immersion of absolute ethyl alcohol. On the condition of pretreatment method A3, γ - Al_2O_3 powder was just immersed in pretreatment agent under normal temperature, the pretreating agent could not erode its surface to form $-\text{OH}$ bond and ZSM-5 could hardly load on its surface. From YFA0, we can notice that mesoporous γ - Al_2O_3 were axiolitic with ladder-shaped striations on them. In contrast to YFA0, the appearance of crystal was also axiohitic in YFA1, but it had a layer of strip-shaped material. In view of XRD patterns, we can preliminarily estimate the materials were ZSM-5 crystal. This fully proved that ZSM-5/ γ - Al_2O_3 composite materials could be synthesized under pretreatment method A1.

3.4 FT-IR Analysis.

Fig.4 demonstrated infrared spectrum of γ - Al_2O_3 under different pretreatment method. As is shown in the Fig. 4-a, there were infrared characteristic peak of γ - Al_2O_3 at 616 cm^{-1} , 1400 cm^{-1} , 1522 cm^{-1} , 1636 cm^{-1} and 3454 cm^{-1} [21]. The peak position of Fig. 4-b、 Fig. 4-c and Fig. 4-d were not quite different. In Fig. 4-b, well-resolved infrared characteristic peak (558 cm^{-1} , 1384 cm^{-1} , 1629 cm^{-1} and 3421 cm^{-1} , wave number) were well matched to γ - Al_2O_3 -type structure. Thus, it can be seen that the functional group of γ - Al_2O_3 did not change after pretreatment. However the infrared peak intensity decreased and red shift occurred, which may be caused by the effect of the pretreatment agent TPAOH. Infrared characteristic peak of TPAOH at 970 cm^{-1} and 1022 cm^{-1} appeared in Fig. 4-b and Fig. 4-c, suggesting partial TPA^+ or OH^- were loaded on γ - Al_2O_3 . An obvious infrared peak at 3620 cm^{-1} were observed in Fig. 4-b and Fig. 4-c, since the infrared characteristic peak of Al-OH bond is $3600\sim 3700\text{ cm}^{-1}$, we speculated that the peak belong to Al-OH and it worked as bridge bond connecting ZSM-5 and form Si-O-Al or Al-O-Al bond, which played a key role in synthesizing ZSM-5/ γ - Al_2O_3 . However neither infrared characteristic peaks of TPAOH nor the peak at 3620 cm^{-1} were observed in Fig. 4-d, indicating that Al-OH were not formed. As the result of XRD patterns have confirmed that ZSM-5/ γ - Al_2O_3 could not synthesized under pretreatment method A3, we can come to a conclusion that Al-OH plays a vital role in the formation of composite materials.



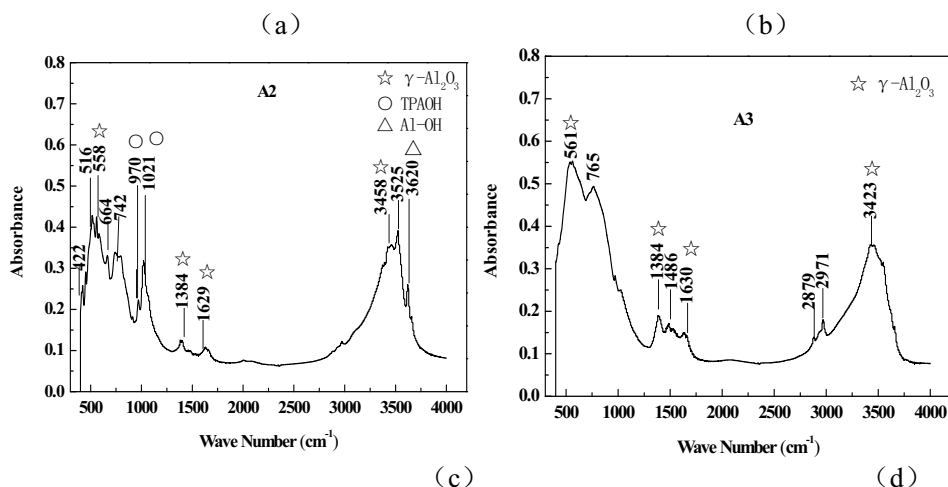


Fig. 4 The infrared spectrum of γ - Al_2O_3 by different pretreatment methods a(without pretreatment); b(pretreatment method A1); c(pretreatment method A2); d(pretreatment method A3)

4 Conclusion

The pretreatment method had great effect on the pore and phase structure of Micro-mesoporous ZSM-5/ γ - Al_2O_3 composite materials. Under the condition of pretreatment method A1, ZSM-5/ γ - Al_2O_3 composite materials can be prepared with superior specific surface area and pore structure along with higher degree of order and axiolitic grain morphology attached to ZSM-5 grains. Al-OH bond can be used as a bridge to connect the ZSM-5, the formation of Si-O-Al or Al-O-Al, ZSM-5 and - Al_2O_3 played a vital role in the composite of Al_2O_3 / ZSM-5. Only under the condition that stable Al-OH bond were formed could the composite materials Al_2O_3 / ZSM-5 be synthesized.

Acknowledgment

This work is supported by National Natural Science Foundation of China (51204179, 51204182), Key Laboratory of Gas and Fire Control for Coal Mines, China University of Mining & Technology, XuZhou, Jiangsu Province, China and The Natural Science Foundation of Jiangsu Province, China (BK20141242).

References

1. M. Rutkowska, L. Chmielarz, D. Macina, et al. Catalytic decomposition and reduction of N_2O over micromesoporous materials containing Beta zeolite nanoparticles, Appl. Catal. B-Environ. 146(2013) 112-122.
2. V.V. Ordonskii, Y.V. Monakhova, E.E. Knyazeva, et al. The physicochemical properties of micro/mesoporous materials prepared by the recrystallization of zeolite BEA, Russ. J. Phys. Chem. A. 83(2009) 1012-1017.

3. L. Gigli, R. Arletti, S. Quartieri, et al. The high thermal stability of the synthetic zeolite K-L: Dehydration mechanism by in situ SR-XRPD experiments, *Microporous Mesoporous Mat.* 177(2013) 8-16.
4. H. Liu, K. Guo, X. Li, et al. Understanding and direct strategy to synthesize hydrothermally stable micro-mesoporous aluminosilicates with largely enhanced acidity, *Microporous Mesoporous Mat.* 188(2014) 108–117.
5. T. Li, A. Duan, Z. Zhen, et al. Synthesis of ordered hierarchically porous L-SBA-15 material and its hydro-upgrading performance for FCC gasoline, *Fuel.* 117(2014) 974-980.
6. D. Zhang, A. Duan, Z. Zhao, et al. Synthesis, characterization and catalytic performance of meso-microporous material Beta-SBA-15-supported NiMo catalysts for hydrodesulfurization of dibenzothiophene. *Catal. Today.* 175(2011) 477-484.
7. Q. Huo, Y. Gong, T. Dou, et al. Novel Micro- and Mesoporous Composite Molecular Sieve Assembled by Zeolite L Nanocrystal and Its Performance for the Hydrodesulfurization (HDS) of Fluidized Catalytic Cracking (FCC) Gasoline, *Energy Fuels.* 24(2010) 3764-3771.
8. H. Liang, X. Guang, L.P. Liu, H.Y. Long, et al. Preparation of highly dispersed desulfurization catalysts and their catalytic performance in hydrodesulfurization of dibenzothiophene, *Chin. J. Catal.* 0(2014): 0-0.
9. B. Saha, A. Khan, H. Ibrahim, et al. Evaluating the performance of non-precious metal based catalysts for sulfur-tolerance during the dry reforming of biogas, *Fuel.* 120(2014) 202–217.
10. H. Quan, D. Tao, Z. Zhen, et al. Synthesis and application of a novel mesoporous zeolite L in the catalyst for the HDS of FCC gasoline, *Appl. Catal. A-Gen.* 381(2010) 101–108.
11. K.R. Kloetstra, H.W. Zandbergen, J.C. Jansen, et al. Overgrowth of mesoporous MCM-41 on faujasite, *Microporous Mesoporous Mat.* 6(1996) 287-293.
12. R.Y. Zhao, J. Liu, Y. Liu, et al. Synthesis and Hydrodesulfurization Evaluation of the Meso-Micropore Composite Zeolite, *Acta Petrol Sin: Pet Process Section.* 26(2010) 657-665.(in Chinese)
13. K.S. Triantafyllidis, A.A. Lappas, I.A. Vasaloss, et al. Gas- oil cracking activity of hydrothermally stable aluminosilicate mesostructures (MSU- S) assembled from zeolite seeds: Effect of the type of framework structure and porosity, *Catal. Today.* 112(2006) 33- 36.
14. K.S. Triantafyllidis, E.F. Iliopoulou, E.V. Antonakou, et al. Hydrothermally stable mesoporous aluminosilicates (MSU- S) assembled from zeolite seeds as catalysts for biomass pyrolysis, *Microporous Mesoporous Mat.* 99(2007) 132- 139.
15. C.J. Vanoers, W.J.J. Stevens, E. Bruijn, et al. Formation of a combined micro and mesoporous material using zeolite Beta nanoparticles, *Microporous Mesoporous Mat.* 120(2009) 29- 34.

16. Y. DI, Y. YU, Y.Y. SUN, et al. Synthesis, characterization, and catalytic properties of stable mesoporous aluminosilicates assembled from preformed zeolite L precursors, *Microporous Mesoporous Mat.* 62(2003) 221- 228.
17. Y.Y. JI, C.Y. WANG, Y.C. ZOU, et al. Design and synthesis of microporous and micro/mesoporous silica materials with excellent adsorption properties via self-assembly of silica species with tetraethyl ammonium in acidic aqueous media, *J. Phys. Chem. C.* 112(2008) 19367- 19371.
18. J.L. Zheng, Y. Zhang, D. WU, et al. Synthesis of hydrothermally stable mesoporous aluminosilicates with tubular morphology from MFI zeolitic precursors and sodium silicates, *Acta Chim. Sinica.* 62(2004) 1357-1361.(in Chinese)
19. J.L. Zheng, S.R. Zhai, D. WU, et al. S + X - I + route to mesostructured materials from fau and beta zeolite precursors: A comparative study of their assembly behaviors in extremely acidic media, *J. Solid State Chem.* 178(2005) 1630-1636.
20. W.J. Kim, S.D. Kim. U.S. Patent 20060111234 A1. (2006)
21. T. Ramanathan, S. Gurudeeban, K. Satyavani, et al. Biomedical potential of silver nanoparticles synthesized from calli cells of *Citrullus colocynthis* (L.) Schrad, *J. Nanobiotechnol.* 9(2011) 43-50.